CHEMISTRY
A EUROPEAN JOURNAL

DOI: 10.1002/chem.200902535

VIP

A Smart Glycol-Directed Nanodevice from Rationally Designed Macroporous Materials

Kun Qian,[a, c] Jingjing Wan,[a, c] Xiaodan Huang,[a] Pengyuan Yang,[a] Baohong Liu,*[a] and Chengzhong Yu*[a, b]

Abstract: We have developed a smart nanodevice for the highly efficient and selective detection of glycoproteins. This polyfunctional device is fabricated through the rational functionalization of macroporous silica foam (MOSF) materials with a boron species (B-MOSF) and amino groups (NH_2-MOSF), and then the integration of MOSF, B-MOSF and NH_2-MOSF materials. In such a device, a macroporous structure with very large-pore sizes (diameters ≈ 100 nm) and high-pore volumes ($> 0.65\ cm^3 g^{-1}$) is advantageous to efficiently fasten the enzymatic reaction. The targeted specific glycopeptides of the products can be selectively isolated and enriched in B-MOSF through the chemo-affinity between boronic acid and glycol groups, while the non-specific peptides are released to the solutions, or further purified by MOSF and NH_2-MOSF, which have opposite charges. As a result, the protein digestion and glycol-peptide isolation can be simultaneously achieved in the functionalized macroporous materials in one step, which is a great advantage compared to conventional multi-procedure and time-consuming techniques.

Keywords: glycolpeptides · glycosylation · macroporous materials · nanotechnology

Introduction

Modern research requires a perfect combination of both nanotechnology and materials science for advanced applications.[1,2] The state-of-the-art nanodevices can be built by utilizing various nano-components, such as nanoparticles, biomolecules and micro/mesoporous materials, with which unique applications have been achieved in many fields, for example, motors[3,4] and sensors.[5,6] Recently, nanoreactor-based devices have received great attention in biological applications and proteome research.[7–9] Substantial progress has been made in the design of nanostructured materials to enhance the proteolysis efficiency,[7,8,10–17] which is a determining step in mass spectrometry (MS) based proteomics.[18,19] Nevertheless, most of the developed devices are limited to promoting enzymatic reactions that take advantage of a pre-immobilized high concentration of enzymes or proteins and are unable to the provide multiple functions, such as rapid proteolysis, selective enrichment and isolation in one device, which are of significant importance for proteome research aimed for modified proteins,[20] for example, glycomics.[21]

The glycosylation of proteins is one of the most common post-translational modifications,[21] which occurs in $\approx 50\,\%$ of all gene products. Glycoproteins are crucial for human physiological and pathological processes in modulating biological functions and activity of proteins.[22,23] Various endeavors have been dedicated to investigate and understand the glycosylation of large-scale proteins by using MS as a basic tool;[21] however, great challenges still exist. The biological complexity of samples can significantly affect the analysis process and glycoproteins at very low abundance are generally difficult to digest and identify.[24,25] Meanwhile, the signals of glycopeptides are frequently suppressed and even lost in noise, owing to the relatively low ionization efficiency of glycopeptides with respect to unmodified peptides and the existence of excessive non-glycosylated peptides, the

[a] K. Qian, J. Wan, X. Huang, Prof. P. Yang, Prof. B. Liu, Prof. C. Yu
Department of Chemistry and Institute of Biomedical Sciences
Shanghai Key Laboratory of Molecular Catalysis
and Innovative Materials
Fudan University, Shanghai 200433 (P.R. China)
Fax: (+86) 21-6564-1740
E-mail: czyu@fudan.edu.cn
bhliu@fudan.edu.cn

[b] Prof. C. Yu
ARC Centre of Excellence for Functional Nanomaterials
and Australian Institute for Bioengineering and Nanotechnology
The University of Queensland, Brisbane, QLD 4072 (Australia)

[c] K. Qian, J. Wan
These authors contributed equally to this work.

Supporting information for this article is available on the WWW under http://dx.doi.org/10.1002/chem.200902535.

latter largely disturbing the identification of glycol-species in the MS analysis.[26,27] Thus urgent demanding rises in the digestion and detection of glycoproteins as well as enrichment and separation of glycopeptides from mixtures.

To date, several strategies have been developed to meet the requirement of isolated and enriched glycol-species with tremendous success, for example, lectin affinity chromatography,[28] hydrazide chemistry,[19] and boronic acid chromatography.[27,29] However, most of the strategies need time-consuming, labor-intensive pre-digestion, post separation and enrichment of the glycol-species with multiple procedures. Currently, there is no reported protocol to integrate the enhanced digestion, enrichment, and isolation of targeted glycol-species in one device, which will be vital for high-throughput glycomics in post-genomic science and clinical research.[25,30]

Compared to the conventional nanoreactors used in digestion,[11,31] macroporous materials with large-pore sizes and high-pore volumes have been shown as superior catalysts to enhance enzymatic reactions.[32–37] It is also demonstrated that by surface modification with TiO_2, functionalized macroporous materials with large surface area can achieve efficient isolation and enrichment of phospho-peptides.[36,38] Therefore, it is expected that by combining the above functions of macroporous materials through careful surface functionalization, novel glycol-directed nanodevices with integrated multi-functions can be fabricated.

Herein, we report a polyfunctional nanodevice targeted for glycol-collection and identification of glycoproteins. The device is based on a glycol-directed nanoreactor, which is obtained by surface functionalization of macroporous silica foam (MOSF) materials[39,40] with a boron species (denoted B-MOSF) and amino groups (denoted NH_2-MOSF), and then the integration of MOSF, B-MOSF and NH_2-MOSF materials. The mechanism of the glycol-directed nanoreactor is shown in Figure 1. The MOSF-based macroporous materials, such as B-MOSF (shown in Figure 1A), can act as catalysts for digestion, owing to the fast enrichment of proteins and enzymes into the nanopores ($\approx$100 nm in diameter), thus the digestion efficiency is greatly enhanced with highly increased local concentrations. Moreover, the specific products of the enzymatic reaction (glycopeptides) are isolated and enriched in situ by B-MOSF, owing to the chemo-affinity between the boronic acid species and the glycol groups,[27,29] while the non-specific peptides are much less captured and/or released to the solution. Importantly, by incorporating NH_2-MOSF and MOSF (with positively and negatively charges, respectively) in addition to B-MOSF in the nanodevice (Figure 1B), the non-specific peptides can be efficiently purified to reduce the sample complexity in a protein mixture. As a result, the protein digestion and glycol-peptide isolation can be efficiently and simultaneously achieved in the functionalized macroporous materials based system, which shows great advantages than the conventional multi-procedure and time-consuming techniques.

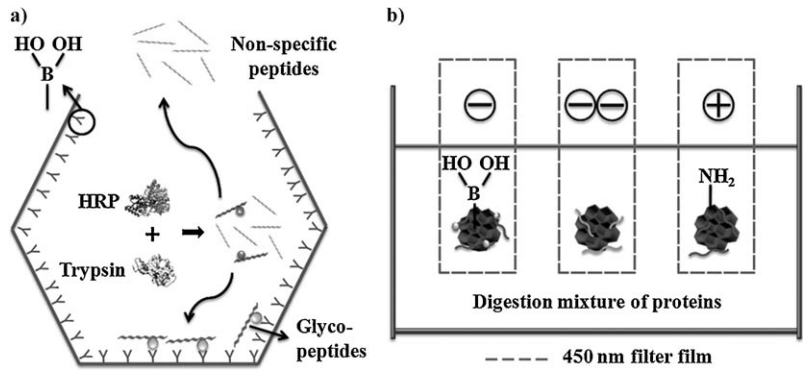

Figure 1. Illustration of the glycol-directed nanodevice. a) B-MOSF material showing both the large macropores favoring enhanced digestion and the functionalized surface designed for glycol-peptides enrichment. b) The integration of B-MOSF, MOSF, and NH_2-MOSF (each sealed individually with $\approx$450 nm microvoid filter film) into the glycol-directed nanodevice to purify non-specific peptides (by MOSF and NH_2-MOSF) and achieve selectively enrichment of glycol-peptides.

Results and Discussion

The porous structures of MOSF materials before and after functionalization are firstly examined. The scanning electron microscopy (SEM) images directly show the foam-like macroporous structures with $\approx$100 nm in pore diameter for pure MOSF and B-MOSF materials (Figure 2a,b). No aggregates can be found in B-MOSF after surface functionalization, indicating that the modification method (see the Experimental Section) has little influence on the foam-like macroporous structure of MOSF. This is also the case for NH_2-MOSF material, the foam structure can be well preserved (Figure S1 in the Supporting Information) after grafting amino groups in the surface of MOSF (see the Experimental Section). The nitrogen sorption analysis is also carried out for MOSF, B-MOSF and NH_2-MOSF materials (Figure S2). The pure MOSF material has a surface area of 241 $m^2 g^{-1}$ and a pore volume of 1.46 $cm^3 g^{-1}$. After the surface functionalization with boronic acid species, the surface area and pore volume of B-MOSF decrease to 102 $m^2 g^{-1}$ and 0.65 $cm^3 g^{-1}$, respectively. Similarly, NH_2-MOSF material has a reduced surface area of 148 $m^2 g^{-1}$ and a pore volume of 0.88 $cm^3 g^{-1}$ after surface modification. The decreases in the surface area and pore volume should be attributed to the functionalization process and the increases in wall thickness. The pore size distribution curves obtained from the adsorption branches of isotherms by the Broekhoff–de Boer (BdB) model show a maximum at $\approx$100, 75 and 80 nm for MOSF, B-MOSF and NH_2-MOSF, respectively (Figure S3). Despite the N_2 sorption analysis cannot accurately measure the sizes of macropores, it is esti-

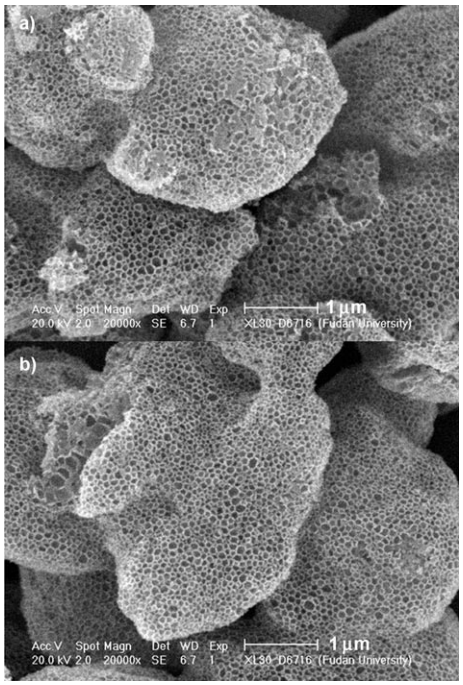

Figure 2. The SEM images of a) pure MOSF and b) B-MOSF.

mated that the macroporous structure after modification is still preserved.

To study the efficiency of surface functionalization, the Fourier transform infrared (FTIR) spectroscopy was employed. The FTIR spectra of MOSF, B-MOSF, as well as the boro-precursor are shown in Figure 3. The FTIR spectrum

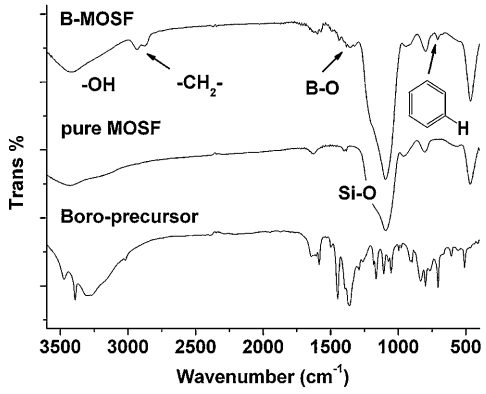

Figure 3. The FTIR spectra of B-MOSF, pure MOSF and Boro-precursor.

of B-MOSF shows double peaks in the region of $\tilde{\nu} \approx 2800\ cm^{-1}$, which can be assigned to the -CH_2- groups of the silane coupling agent (see the Experimental Section). Such characteristic peaks cannot be found in the FTIR spectrum of pure MOSF. Moreover, compared to the FTIR spectrum of MOSF, two additional bands are observed in that of B-MOSF, one at $\tilde{\nu} 708\ cm^{-1}$ and the other broad band centered at $\tilde{\nu} \approx 1352\ cm^{-1}$, which can be attributed to the addition of the boro-benzene and boronic acid species in boro-precursor, respectively,[27,29] indicating that the boron species are present on the surface of B-MOSF. We also examine the obtained B-MOSF by solid state magic angle spinning (MAS) ^{13}C nuclear magnetic resonance (NMR) spectrometry, as displayed in Figure S4. The existence of O-CH_2 groups is proved by the observation of peaks centered at $\delta = 58$ and 72 ppm.[41–43] The peaks at $\delta = 8$ and 24 ppm belong to Si–C and -CH_2- groups respectively,[41–44] whereas the signals at $\delta = 128$ and 148 ppm are attributed to the resonances of carbons in the benzene ring for the boronic precursor, consistent with FTIR results.[42,44]

The zeta potential measurement was carried out for three materials in the ammonium bicarbonate buffer solution (pH ≈ 8). As shown in Figure 4, the zeta potential of pure MOSF

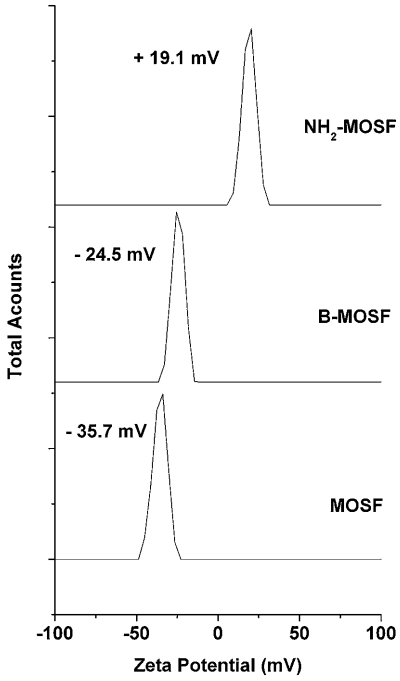

Figure 4. The zeta potential distributions of pure MOSF, B-MOSF and NH_2-MOSF.

material is −35.7 mV, consistent with the low isoelectric point of silica (pI ≈ 2). After surface modification, B-MOSF has an increased zeta potential of −24.5 mV, which can be explained by that Si–OHs are substituted by B–OHs. While for the NH_2-MOSF material, the zeta potential is measured to be +19.1 mV. Only one narrow peak is observed for both B-MOSF and NH_2-MOSF materials, whereas the peak at −35.7 mV for pure silica cannot be observed after surface modification. The above zeta potential measurements have displayed that the boron species and amino species have been successfully functionalized onto the pure silica surface of MOSF for B-MOSF and NH_2-MOSF respectively, in agreement with nitrogen sorption, FTIR and NMR results.

To demonstrate the functions of glycol-directed nanodevice constructed by different MOSF materials, we firstly use B-MOSF as an example to show that the MOSF-type mate-

rials have high enzyme/protein immobilization capacity and can thus greatly enhance the enzymatic reactions. For trypsin, an enzyme universally employed in the digestion system, ≈95% of the maximum adsorption amount can be achieved within one minute (as shown in Figure 5). Moreover, the immobilization capacity of trypsin is 370 mg (g·B-MOSF)$^{-1}$. In the case of a standard glycoprotein, horseradish peroxidase (HRP), the immobilization capacity adsorbed in B-MOSF is 310 mg g(B-MOSF)$^{-1}$ and the maximum immobilization capacity is also obtained in less than 1 min (Figure 5). In a typical digest system, the concentration of the protein (HRP) is as low as 0.02 mg mL^{-1}, thus it is not convenient to measure the immobilization capacity of HRP in B-MOSF at such a low concentrations. Nevertheless, considering the large immobilization capacity of HRP in B-MOSF (310 mg g^{-1}) measured at a higher HRP concentration (1 mg mL^{-1}), it can be roughly estimated that a B-MOSF concentration of ≈0.06 mg mL^{-1} should be used to immobilize HRP (0.02 mg mL^{-1}), thus in 1 mL of digest solution, the weight ratio of HRP to B-MOSF is 0.02 mg:0.06 mg, close to that of 310 mg (HRP) g(B-MOSF)$^{-1}$ measured in the immobilization test. In our further digest experiments, the B-MOSF concentration is increased to 0.13 mg mL^{-1}, to immobilize the maximum amount of HRP into B-MOSF. The pore volume of B-MOSF is 0.65 cm^3 g^{-1}, thus in 1 mL of digestion solution, the pore volume contributed by 0.13 mg of B-MOSF is 84.5×10^{-6} cm^3. Assuming that the majority of glycoprotein can be quickly absorbed from the solution into the macropores of B-MOSF, a concentration increase of ≈1, 1000 times can be calculated (from 0.02 mg mL^{-1} in solution to 220 mg mL^{-1} in macropores for HRP). Because the immobilization capacity of trypsin in B-MOSF is also high (370 mg g^{-1}) and the weight ratio of trypsin to HRP is 1:30, the relatively smaller amount of trypsin can also be entrapped quickly into B-MOSF. It is expected that the in situ enrichment of proteins and enzymes into the nanopores of these materials can significantly increase the effective collision between biomolecules and thus enhance the enzymatic reactions.

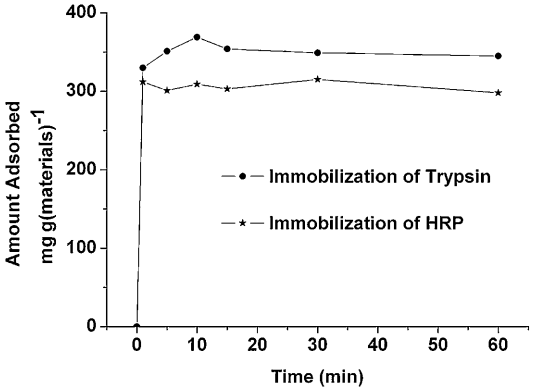

Figure 5. Immobilization of trypsin and HRP to B-MOSF as a function of time.

The advantage of using B-MOSF as a catalyst to improve the HRP digestion efficiency can be directly seen by means of the matrix-assisted laser desorption/ionization time-of-flight mass spectrometry (MALDI-TOF MS). It has been well characterized that HRP has nine glycosylation sites, and most of the glycopeptides from HRP are located at the mass weight range above 2000, whereas almost all the non-glycopeptides are located below 2000. The peptides mass fingerprint (PMF) spectra of HRP (20 ng μL^{-1}) digested in-solution and in the presence of B-MOSF are shown in Figure 6 consuming 2.5 pmol digests. The mass spectrum obtained through in-solution digestion shows that proteolysis is incomplete in 30 min (Figure 6a,b). Only 3 glycopeptides as well as 3 non-glycopeptides are identified, while the resolution of both glycopeptides and non-glycopeptides is very

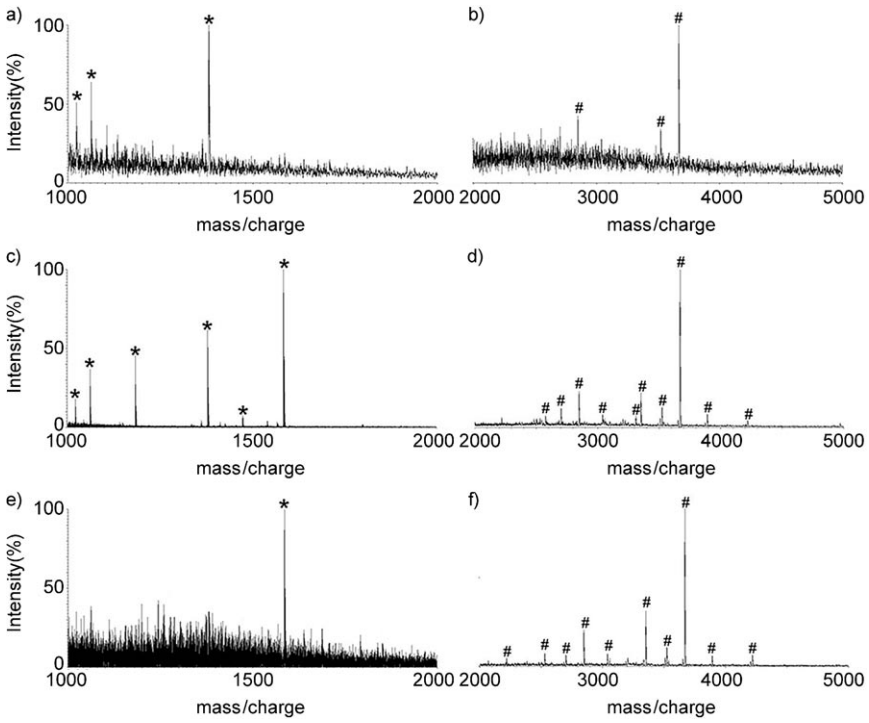

Figure 6. PMF spectra of 20 ng μL^{-1} HRP proteolysis products from a,b) 30 min in-solution digestion, c,d) 30 min B-MOSF catalyzed digestion and e,f) the elution buffer from the B-MOSF for digestion and isolation in one step after 30 min. The star stands for the non-glycopeptide and # stands for the glycopeptide.

low. In the presence of B-MOSF, 6 non-glycol-peptides and 10 glycol-peptides have been identified with high signal-to-noise (S/N) ratios in a similar in-solution digestion system at 30 min (Figure 6c,d), indicating that the enzymatic reaction rate has been greatly accelerated in the presence of B-MOSF as a catalyst. For comparison, the overnight in-solution (12 h) digestion method yields 10 non-glycol-peptides and 6 glycol-peptides identified (Figure S5): Not only is the number of identified glycol-peptides less compared to the B-MOSF catalyzed digestion at 30 min, but also the S/N ratio is less resolved (compared Figure S3 to Figure 6c,d). Our results have shown that even at a very low HRP concentration (2 ng μL^{-1}), the digestion efficiency can be highly enhanced in 30 min in the presence of B-MOSF (Figure S6).

Secondly we demonstrate that B-MOSF can also be used to enrich glycopeptides after efficient in situ digestion. A selective extraction of the glycol-species is realized by means of a simple elution of B-MOSF after digestion. As shown in Figure 6e–f, almost all the non-glycopeptides are released with only one weak, non-glycopeptide signal observed in the elution. In the case of the glycopeptides, 10 glycopeptides are detected in the elution with high S/N ratios. By comparing Figure 6e,f and c,d, it is seen that the relative distribution of glycopeptides to non-glycopeptides is much higher within B-MOSF compared to an in-solution digest, indicating that the glycopeptides generated from the in situ digestion can be preferentially adsorbed into B-MOSF while the non-glycopeptides are released to solution. For comparison, pure MOSF was also employed in the above analysis. After digestion and isolation under exactly the same conditions, only two glycopeptides with very low S/N ratios are found in the elution of MOSF without any modification (Figure S7), indicating the non-selectivity of the pure silica materials. Therefore, the preferential capture of glycopeptides in B-MOSF should be attributed to its functionalized surfaces.

Considering the complexity of the samples, the various functions of B-MOSF were further investigated by using a protein mixture of HRP together with a non-glycoprotein, bovine serum A (BSA, see the Experimental Section). Figure 7a,b show the PMF results obtained by means of an in-solution digestion in 30 min. 17 Non-glycopeptides are observed, whereas only 5 glycopeptides can be found with less-resolved S/N ratios. In the presence of B-MOSF, it is noted that there are still 15 non-glycopeptides detected with relatively decreased S/N ratios while the signals of the glycopeptides are suppressed (Figure 7c,d). The results are attributed to the existence of a large amount of non-specific proteins and thus generated non-specific peptides, which reduce the preferential interaction of boronic acid species with glycopeptides and thus decrease the selectivity of B-MOSF towards glycopeptides.

To design a selective glycol-directed nanodevice with high tolerance to non-specific species in complex systems, we fabricated a system that consists of B-MOSF, NH_2-MOSF and MOSF (Figure 1B). All MOSF-type materials are sealed separately in $\approx$450 nm microvoid filter film. With this design, each material (e.g., B-MOSF) can be easily taken out of the solution for subsequent washing and elution treatments, while centrifugation is avoided. Additionally, the relatively large void size of the filter film is easy for the transportation of both proteins and peptides in-and-out of the solution to MOSF materials. As shown in Figure 7e–f, 10 glycopeptides have been successfully identified with high S/N ratios with such device from the elution of B-MOSF after 30 min of digestion, whereas the non-specific adsorption of non-glycopeptides has been greatly reduced with only three observed. To further demonstrate the mechanism of the nanodevice, the elutions of isolated MOSF and NH_2-MOSF were also detected. It is noted that 14 non-specific peptides

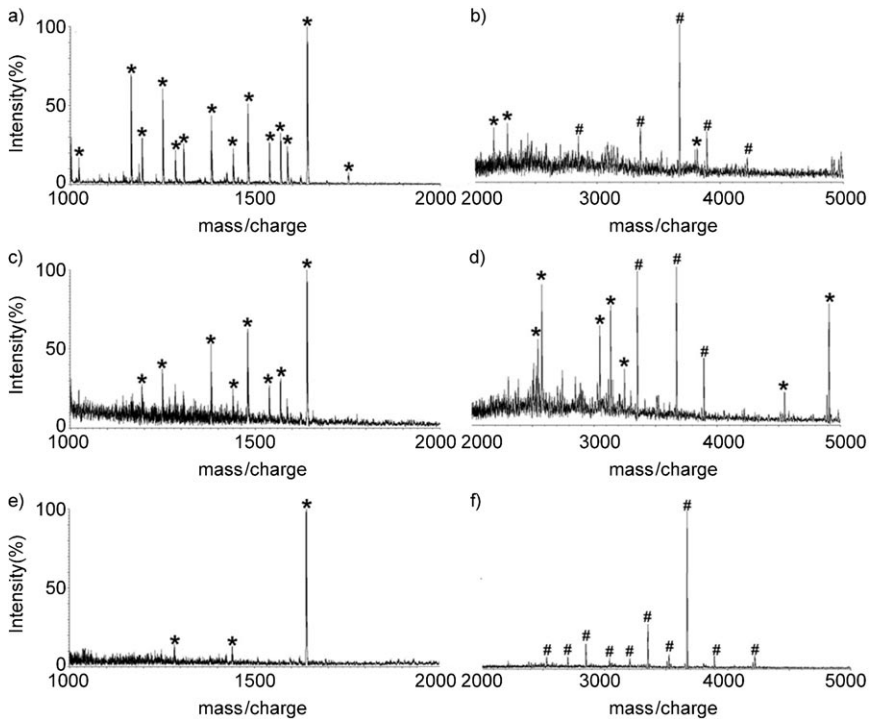

Figure 7. PMF spectra of mixture of BSA and HRP at the ratio of 1:1 (mol/mol) from a,b) bulk solutions in 30 min, c,d) elution of B-MOSFs with only B-MOSF used for digestion and isolation after 30 min, and e,f) elution of B-MOSFs with B-MOSF, MOSF and NH_2-MOSF used for digestion, isolation and purification after 30 min, the concentration of HRP was fixed to 20 ng μL^{-1}. The star stands for the non-glycopeptide and # stands for the glycopeptide.

are found in the elution of the isolated MOSF with no trace of glycopeptide (Figure S8 A). As for NH_2-MOSF, 13 non-specific peptides are found and only one weak peak of glycopeptide is observed (Figure S8 B). It can be concluded that a majority of non-specific peptides are purified by MOSF and NH_2-MOSF materials, which can effectively enhance the selectivity of B-MOSF towards glycopeptides.

Conclusions

In conclusion, we have designed a polyfunctional, easily-operated nanodevice targeted for highly efficient, selective and sensitive glycoprotein analysis. By rational design and surface modification of macroporous materials, the integrated system can achieve fast digestion, selective enrichment of targeted glycopeptides, and purification of non-glycopeptides simultaneously, which possesses advantages than the conventional multi-procedure and time-consuming techniques. It is anticipated that the concept used in this fabrication of glycol-directed nanodevice can be further employed to design other types of targeted systems in modern proteome research, biosensors and bio-separations.

Experimental Section

Chemicals: Tetramethoxysilane (TMOS), $EO_{20}PO_{70}EO_{20}$ [denoted P123, where EO is poly(ethylene oxide) and PO is poly(propylene oxide)], 3-aminopropyltriethoxysilane (APTS), 3-Aminophenylboronic acid (APBA), 3-glycidoxypropyltrimethoxysilane (GLYMO) and ammonium bicarbonate were purchased from Aldrich. Trypsin (from bovine pancreas), horseradish peroxidase (HRP) and bovine serum A (BSA) were obtained from Sigma. 2,5-dihydroxybenzoic acid (DHB, 99.9%), acetonitrile (ACN, 99.9%) and trifluoroacetic acid (TFA, 99.8%) were purchased from Merck. All reagents were used as received without further purification. The microvoid filter was purchased from Shanghai Xinya Purifier Devices Factory. Deionized water (18.4 MΩ cm) used for all experiments was obtained from a Milli-Q system (Millipore, Bedford, MA, USA).

Synthesis, modification and characterization of porous materials: Typically the synthesis of MOSF was as previously reported by us,[39] and was carried out at 35 °C in a buffer solution (pH ≈ 5) with TMOS as a silica source and P123 as a template. The final MOSF products were obtained after baking at 550 °C for 5 h. A published method was adapted for the modification with amino groups,[45] dried MOSF (0.2 g) was suspended in 30 mL toluene and an excess of APTS (2 mL) was added. The mixture was stirred at 110 °C for one day. Then the slurry was filtered and washed with dichloromethane and ethanol for 3 times, and finally dried at 70 °C. The modification of MOSF with boron species was according to a reported method.[27] First APBA was blended with GLYMO at a molar ratio of 1:1 to conduct a coupling process (GLYMO-APBA).[27] Then MOSF was grafted with the above coupled agent to form the B-MOSF. In detail, APBA (34 mg) was dissolved in water (30 g) and the pH was adjusted to ≈9. Then GLYMO (58 mg) was added and stirred for 8 h at 40 °C. The slurry was centrifuged and then dried MOSF (50 mg) was dispersed in the clear solution obtained. The mixture was stirred for 24 h at 70 °C. The resulting pink powder was collected and washed by water and dried at room temperature. SEM images were taken by a Philips XL30 microscope. Nitrogen sorption isotherms of samples were recorded by using a Quantachrome's Quadrasorb SI analyzer at 77 K. A zeta-potential meter (Malvern Zetasizer Nano) was used to measure the zeta potentials of the materials at 25 °C in the ammonium bicarbonate buffer (pH ≈ 8). The infrared spectra were obtained by using a FT-IR360 manufactured by Nicolet. The MAS ^{13}C NMR spectra were recorded by using a Bruker DSX 300 NMR spectrometer.

Immobilization of proteins/enzymes into the B-MOSF: Kinetic experiments to determine the amount of trypsin and HRP adsorbed into B-MOSF as a function of contact time were conducted by mixing 4 mL of 1.0 mg mL^{-1} protein solution (25 mM NH_4HCO_3 buffer at pH ≈ 8) with 5 mg of B-MOSF under stirring at 298 K. The immobilization capacity of proteins and enzymes in materials were evaluated by measuring protein adsorption amounts. The mixtures were stirred for different time and the adsorbed amount was measured using a difference method with protein concentrations determined before and after adsorption by UV absorption at $\lambda = 280$ nm by using a V-550 UV/Vis spectrophotometer.

Analysis of performance of the glycol-directed nanodevice/reactor by using MS: In-solution digestion was performed according to the widely used method. Amounts of horseradish peroxidase (HRP) were dissolved (2, 20 ng μL^{-1}) in ammonium bicarbonate buffer (50 mM, pH ≈ 8) with trypsin at an enzyme/substrate ratio of 1:30 (w/w). To perform one step experiment, a suspension of boric modified materials (20 mg mL^{-1}, 2 μL) was added to the above mentioned solution (300 μL). The mixed solution was then vibrated at 37 °C for 30 min. After that, the mixture was centrifuged to remove the supernatant, and the deposits were washed with ammonium bicarbonate buffer (50 mM, pH ≈ 8) twice. Then, the rinsed materials were redispersed in 10 μL 1% TFA/50% ACN aqueous solution (v/v) to elute the digested glycopeptides. For the selectivity test, 10 μL of MOSF, NH_2-MOSF and B-MOSF suspension (20 mg mL^{-1}) were isolated independently by 450 nm microvoid filter films and immersed in 10 mL digestion mixture of HRP and BSA at molar ratio 1:1 (20 ng μL^{-1}) with trypsin at an enzyme/substrate ratio of 1:30 (w/w) for 30 min. The B-MOSF was washed and eluted as the above mentioned. Finally, 0.5 μL eluted supernatant was deposited on the MALDI plate, after evaporation, 0.5 μL matrix (DHB, at 12.5 mg mL^{-1} in ACN/water/TFA, 30/69.9/0.1% (v/v)) was added and followed by MS analysis. Deionized water (18.4 MΩ cm) was used for all experiments obtained from a Milli-Q system (Millipore, Bedford, MA, USA). All mass spectra were acquired by using a MALDI AXIMA QIT (Shimadzu Biotech, Japan).

Acknowledgements

This work is supported by 973 Program (2010CB226901, 2007CB714506), NSFC (20573021, 20775016, 20925517, 20735005), SLADP (B108, B109), STC of Shanghai (08DZ2270500, 09JC1402600), Shuguang 06SG02, the Ministry of Education of China (20060246010), FANEDD (200423), and Australia Research Council.

[1] M. T. Björk, H. Schmid, J. Knoch, H. Riel, W. Riess, *Nat. Nanotechnol.* **2009**, *4*, 103–107.
[2] H. P. Wang, J. K. Keum, A. Hiltner, E. Baer, B. Freeman, A. Rozanski, A. Galeski, *Science* **2009**, *323*, 757–760.
[3] Q. He, L. Duan, W. Qi, K. W. Wang, Y. Cui, X. H. Yan, J. B. Li, *Adv. Mater.* **2008**, *20*, 2933–2937.
[4] C. T. Lin, M. T. Kao, K. Kurabayashi, E. Meyhofer, *Small* **2006**, *2*, 281–287.
[5] K. Jensen, K. Kim, A. Zettl, *Nat. Nanotechnol.* **2008**, *3*, 533–537.
[6] M. W. Li, R. B. Bhiladvala, T. J. Morrow, J. A. Sioss, K. K. Lew, J. M. Redwing, C. D. Keating, T. S. Mayer, *Nat. Nanotechnol.* **2008**, *3*, 88–92.
[7] M. Comellas-Aragonès, H. Engelkamp, V. I. Claessen, N. Sommerdijk, A. E. Rowan, P. C. M. Christianen, J. C. Maan, B. J. M. Verduin, J. Cornelissen, R. J. M. Nolte, *Nat. Nanotechnol.* **2007**, *2*, 635–639.
[8] N. Bruns, J. C. Tiller, *Nano Lett.* **2005**, *5*, 45–48.
[9] S. Y. Lee, X. Y. Gao, H. Matsui, *J. Am. Chem. Soc.* **2007**, *129*, 2954–2958.
[10] J. Fan, W. Q. Shui, P. Y. Yang, X. Y. Wang, Y. M. Xu, H. H. Wang, X. Chen, D. Y. Zhao, *Chem. Eur. J.* **2005**, *11*, 5391–5396.

[11] L. Qiao, Y. Liu, S. P. Hudson, P. Y. Yang, E. Magner, B. H. Liu, *Chem. Eur. J.* **2008**, *14*, 151–157.
[12] P. A. Sigala, D. A. Kraut, J. M. M. Caaveiro, B. Pybus, E. A. Ruben, D. Ringe, G. A. Petsko, D. Herschlag, *J. Am. Chem. Soc.* **2008**, *130*, 13696–13708.
[13] C. H. Lei, Y. Shin, J. Liu, E. J. Ackerman, *Nano Lett.* **2007**, *7*, 1050–1053.
[14] W. Shang, J. H. Nuffer, J. S. Dordick, R. W. Siegel, *Nano Lett.* **2007**, *7*, 1991–1995.
[15] Y. Liu, H. J. Lu, W. Zhong, P. Y. Song, J. L. Kong, P. Y. Yang, H. H. Girault, B. H. Liu, *Anal. Chem.* **2006**, *78*, 801–808.
[16] Y. Liu, Y. Xue, J. Ji, X. Chen, J. Kong, P. Y. Yang, H. H. Girault, B. H. Liu, *Mol. Cell. Proteomics* **2007**, *6*, 1428–1436.
[17] Y. Liu, W. Zhong, S. Meng, J. L. Kong, H. J. Lu, P. Y. Yang, H. H. Girault, B. H. Liu, *Chem. Eur. J.* **2006**, *12*, 6585–6591.
[18] B. F. Cravatt, G. M. Simon, J. R. Yates, *Nature* **2007**, *450*, 991–1000.
[19] Y. A. Tian, Y. Zhou, S. Elliott, R. Aebersold, H. Zhang, *Nat. Protoc.* **2007**, *2*, 334–339.
[20] R. Aebersold, M. Mann, *Nature* **2003**, *422*, 198–207.
[21] J. Zaia, *Chem. Biol.* **2008**, *15*, 881–892.
[22] R. Fujiki, T. Chikanishi, W. Hashiba, H. Ito, I. Takada, R. G. Roeder, H. Kitagawa, S. Kato, *Nature* **2009**, *459*, 455–459.
[23] M. G. Vander Heiden, L. C. Cantley, C. B. Thompson, *Science* **2009**, *324*, 1029–1033.
[24] B. Y. Xia, Z. S. Kawar, T. Z. Ju, R. A. Alvarez, G. P. Sachdev, R. D. Cummings, *Nat. Methods* **2005**, *2*, 845–850.
[25] V. Kulasingam, E. P. Diamandis, *Nat. Clin. Pract. Oncol.* **2008**, *5*, 588–599.
[26] W. Ding, J. J. Hill, J. Kelly, *Anal. Chem.* **2007**, *79*, 8891–8899.
[27] Y. W. Xu, Z. X. Wu, L. J. Zhang, H. J. Lu, P. Y. Yang, P. A. Webley, D. Y. Zhao, *Anal. Chem.* **2009**, *81*, 503–508.
[28] H. Kaji, Y. Yamauchi, N. Takahashi, T. Isobe, *Nat. Protoc.* **2007**, *1*, 3019–3027.
[29] W. S. Yeap, Y. Y. Tan, K. P. Loh, *Anal. Chem.* **2008**, *80*, 4659–4665.
[30] N. Blow, *Nat. Methods* **2008**, *5*, 741–747.
[31] S. Hudson, J. Cooney, E. Magner, *Angew. Chem.* **2008**, *120*, 8710–8723; *Angew. Chem. Int. Ed.* **2008**, *47*, 8582–8594.
[32] K. Qian, J. Wan, L. Qiao, X. Huang, J. Tang, Y. Wang, J. Kong, P. Yang, C. Yu, B. Liu, *Anal. Chem.* **2009**, *81*, 5749–5756.
[33] K. Nakanishi, Y. Kobayashi, T. Amatani, K. Hirao, T. Kodaira, *Chem. Mater.* **2004**, *16*, 3652–3658.
[34] K. Nakanishi, N. Tanaka, *Acc. Chem. Res.* **2007**, *40*, 863–873.
[35] N. Brun, B. Julian-Lopez, P. Hesemann, G. Laurent, H. Deleuze, C. Sanchez, M. F. Achard, R. Backov, *Chem. Mater.* **2008**, *20*, 7117–7129.
[36] K. Qian, J. Wan, F. Liu, H. H. Girault, B. H. Liu, C. Z. Yu, *ACS Nano* **2009**, *3*, 3656–3662.
[37] Y. H. Zhang, Y. Liu, J. L. Kong, P. Y. Yang, Y. Tang, B. H. Liu, *Small* **2006**, *2*, 1170–1173.
[38] J. J. Wan, K. Qian, L. Qiao, Y. H. Wang, J. L. Kong, P. Y. Yang, B. H. Liu, C. Z. Yu, *Chem. Eur. J.* **2009**, *15*, 2504–2508.
[39] H. N. Wang, X. F. Zhou, M. H. Yu, Y. H. Wang, L. Han, J. Zhang, P. Yuan, G. Auchterlonie, J. Zou, C. Z. Yu, *J. Am. Chem. Soc.* **2006**, *128*, 15992–15993.
[40] P. Yuan, X. F. Zhou, H. N. Wang, N. A. Liu, Y. F. Hu, G. J. Auchterlonie, J. Drennan, X. D. Yao, G. Q. Lu, J. Zou, C. Z. Yu, *Small* **2009**, *5*, 377–382.
[41] M. A. Wahab, H. Hussain, C. He, *Langmuir* **2009**, *25*, 4743–4750.
[42] S. Bachmann, H. Y. Wang, K. Albert, R. Partch, *J. Colloid Interface Sci.* **2007**, *309*, 169–175.
[43] S. Budi Hartono, S. Z. Qiao, K. Jack, B. P. Ladewig, Z. Hao, G. Q. M. Lu, *Langmuir* **2009**, *25*, 6413–6424.
[44] E. B. Cho, D. Kim, M. Jaroniec, *Langmuir* **2007**, *23*, 11844–11849.
[45] A. B. Descalzo, D. Jimenez, M. D. Marcos, R. Martinez-Manez, J. Soto, J. El Haskouri, C. Guillem, D. Beltran, P. Amoros, M. V. Borrachero, *Adv. Mater.* **2002**, *14*, 966–969.

Received: September 15, 2009
Published online: December 18, 2009

